

GZK Photons Above 10 EeV

Graciela Gelmini^a, Oleg Kalashev^{a,b} and Dmitry V. Semikoz^{b,c}

^a Department of Physics and Astronomy, UCLA, Los Angeles, CA 90095-1547, USA

^b INR RAS, 60th October Anniversary pr. 7a, 117312 Moscow, Russia

^c APC, College de France, 11 pl. Marcelin Berthelot, Paris 75005, France

Abstract. We calculate the flux of “GZK-photons”, namely the flux of photons produced by extragalactic nucleons through the resonant photoproduction of pions, the so called GZK effect. This flux depends on the UHECR spectrum on Earth, of the spectrum of nucleons emitted at the sources, which we characterize by its slope and maximum energy, on the distribution of sources and on the intervening cosmological backgrounds, in particular the magnetic field and radio backgrounds. For the first time we calculate the GZK photons produced by nuclei. We calculate the possible range of the GZK photon fraction of the total UHECR flux for the AGASA and the HiRes spectra. We find that for nucleons produced at the sources it could be as large as a few % and as low as 10^{-4} above 10^{19} eV. For nuclei produced at the sources the maximum photon fraction is a factor of 2 to 3 times smaller above 10^{19} eV but the minimum could be much smaller than for nucleons. We also comment on cosmogenic neutrino fluxes.

PACS numbers: 98.70.Sa

1. Introduction

The cosmic rays with energies beyond the Greisen-Zatsepin-Kuzmin (GZK) cutoff [1] at 4×10^{19} eV present a challenging outstanding puzzle in astroparticle physics and cosmology [2, 3, 4, 5]. Nucleons cannot be significantly deflected by the magnetic fields of our galaxy for energies above the “ankle”, i.e. above $10^{18.5}$ eV. This and the absence of a correlation of arrival directions with the galactic plane indicate that, if nucleons are the primary particles of the ultra high energy cosmic rays (UHECR), these nucleons should be of extragalactic origin. However, nucleons as well as photons with energies above 5×10^{19} eV could not reach Earth from a distance beyond 50 to 100 Mpc [6, 7] and no sources have been so far found within this distance. Nucleons scatter off the cosmic microwave background (CMB) photons with a resonant photoproduction of pions $p\gamma \rightarrow \Delta^* \rightarrow N\pi$, where the pion carries away $\sim 20\%$ of the original nucleon energy. The mean free path for this reaction is only 6 Mpc. Photons with comparable energy pair-produce electrons and positrons on the radio background and the uncertainty in this background translates into uncertainty in the photon energy-attenuation length.

Intervening sheets of large scale intense extra galactic magnetic fields (EGMF), with intensities $B \sim 0.1 - 1 \times 10^{-6}$ G, could provide sufficient angular deflection for protons to explain the lack of observed sources in the directions of arrival of UHECR. However, recent realistic simulations of the expected large scale EGMF, show that strong deflections could only occur when particles cross galaxy clusters. Except in the regions close to the Virgo, Perseus and Coma clusters the magnetic fields are not larger than 3×10^{-11} G [8] and the deflections expected are not important (however see Ref. [9]).

Whether particles can be emitted with the necessary energies by astrophysical accelerators, such as active galactic nuclei, jets or extended lobes of radio galaxies, or even extended object such as colliding galaxies and clusters of galaxies, is still an open question. The size and possible magnetic and electric fields of these astrophysical sites make it plausible for them to produce UHECR at most up to energies of 10^{21} eV. Larger emission energies would require a reconsideration of possible acceleration models or sites.

Heavy nuclei are an interesting possibility for UHECR primaries, since they could be produced at the sources with larger maximum energies (proportional to their charges) and would more easily be deflected by intervening magnetic fields. On the other hand, both AGASA and HiRes data favor a dominance of light hadrons, consistent with being all protons, in the composition of UHECR above 10^{19} eV. These data are consistent with models in which all UHECR above 10^{18} eV are due to extragalactic protons [10].

A galactic component of the UHECR flux, which could be important up to energies 10^{19} eV, should consist of heavy nuclei, given the lack of correlation with the galactic plane of events at this energy (outside the galactic plane galactic protons would be deflected by a maximum of $15-20^\circ$ at this energies [11]).

The GZK cutoff at 4×10^{19} eV seems not to be present in the data of the AGASA ground array [2] but it appears in the data of the HiRes air fluorescence detector [4, 5].

This controversy can be addressed by the Pierre Auger Observatory [12], a hybrid combination of charged particles detectors and fluorescence telescopes, as it continues to accumulate data.

The GZK process produces pions. From the decay of π^\pm one obtains neutrinos. These “cosmogenic neutrinos” (sometimes called these days “GZK neutrinos”) have been extensively studied, from 1969 [13] onward (see for example [14, 15] and references therein), and constitute one of the main high energy signals expected in neutrino telescopes, such as ICECUBE [16] ANITA [17] and SALSA [18] or space based observatories such as EUSO [19] and OWL [20]. From the decay of π^0 we obtain photons, “GZK photons”, each with about 0.1 of the original proton energy, which have been known to be a subdominant component of the UHECR since the work of Wdowczyk *et al.* in the early 1970’s [21]. In 1990 it was suggested that if the extragalactic radio background and magnetic fields are small ($B < 3 \times 10^{-11}$ G) GZK photons could dominate over protons and explain the super-GZK events [22]. The dependence of the GZK photon flux on extragalactic magnetic fields was later studied in Ref. [23]. The argument of Ref. [22] and its dependence on extragalactic magnetic fields was again discussed [24] in connection with the possible correlation of UHECR arrival directions with BL Lacertae objects [25]. However, to our knowledge, the first complete study of the expected fluxes of GZK photons, including their dependence on the initial proton fluxes, distribution of proton sources and UHECR spectrum, besides intervening backgrounds, was done in Ref. [26], and completed here with an improved statistical analysis (first used in Ref. [27]).

With the advent of the Pierre Auger Observatory, we expect to have in the near future the high statistic data that may allow to study a subdominant component of UHECR consisting of photons [28, 29]. Auger has already set bounds on the photon fraction above 10^{19} eV [30] and better bounds are expected soon. The GZK photons provide a complementary handle to GZK neutrinos and other signatures to try to determine the spectrum and composition of the UHECR. The flux of GZK photons is necessarily correlated with the flux of cosmogenic neutrinos, although the former is affected by the radio background and EGMF values which do not affect the latter. Auger will hopefully see photons or place a limit on the photon fraction at the level of a few % or below. If complemented by an extended northern array [31], a sensitivity level of below 0.1% could be reached within a few years of full operation [29]. Here we would like to address the physical implications of such detection or limits.

In this paper we fit the assumed UHECR spectrum above 4×10^{19} eV solely with primary nucleons and the GZK photons they produce. The GZK photon flux depends on the UHECR spectrum assumed, the slope and maximum energy of the primary nucleon flux, the distribution of sources and the intervening backgrounds [26]. We take a phenomenological approach in choosing the range of the several relevant parameters which determine the GZK photon flux, namely we take for each of them a range of values mentioned in the literature, without attempting to assign them to particular sources or acceleration mechanisms. We also study here for the first time the GZK photon flux

produced if nuclei are emitted at the sources. In this case we fit the AGASA or HiRes spectrum above 4×10^{19} eV with the nuclei and nucleons resulting from the disintegration of the primary nuclei and the GZK photons they produce. To compare them with the ratios produced by pure protons, we present the GZK photon ratios in the simplified case in which either only He, or O or Fe would be produced at the sources.

The ankle in the UHECR spectrum at energies 10^{18} eV - 10^{19} eV can be explained either by e^\pm production by extragalactic protons or by a change from one component of the UHECR spectrum to another. The latter explanation assumes the existence of a low energy component (LEC) when necessary to fit the assumed UHECR at energies below 10^{19} eV. This LEC can be dominated by galactic Fe or by a different population of lower energy extragalactic nucleons. This last possibility can still be consistent with the proton-dominated composition observed by HiRes. Here we do not address the issue of what the LEC is. We only assume that, if it exists, it becomes negligible at energies above 4×10^{19} eV, the energy above which we fit the data. In addition we impose that the spectrum we predict is never above the measured spectrum at energies below 4×10^{19} eV. The LEC in any event does not contribute to the flux of GZK photons since it is important at energies under the threshold for photo-pion production.

In order to find the expected range of the GZK photon flux, we fit either the AGASA or the HiRes data above 4×10^{19} eV either minimizing or maximizing the number of GZK protons produced. We find (see Figs. 6 and 7) that (assuming exclusively protons are emitted at the sources) the GZK photon fraction of the total integrated UHECR flux could reach a few % above 10^{19} eV and 10% above 10^{20} eV, or be between one (for AGASA) and several (for HiRes) orders of magnitude smaller, under the level that could be detected at Auger South alone. In fact, we find (as in Ref. [27] and Ref. [32]) that the photon fraction in cosmic rays at energies above 10^{19} eV could be as low as $O(10^{-4})$. Photon fluxes so small could only be detected in future experiments like Auger North plus South [31, 29], EUSO [19] and OWL [20]. In Fig. 6 a zero minimum distance to the sources is assumed. i.e. a minimum distance much smaller than all relevant interaction lengths. In Fig. 7 a minimum distance to the sources of 50 Mpc (actually a minimum redshift 0.01) is assumed. As clearly shown in Figs. 4 (where $z_{\min} = 0$) and Fig. 5 (where z_{\min} is allowed to vary between 0 and 0.01) the GZK photon fractions depend strongly on the maximum energy of the protons initially emitted at the sources. Just for comparison in Figs. 4 and 6 we also show the range of GZK-photon fractions expected if purely He or purely Fe nuclei (also O in Figs. 4) were emitted at the sources, and in these cases the maximum GZK photon fractions expected are smaller.

The detection of GZK photons would open the way for UHECR photon astronomy. The detection of a larger photon flux than expected for GZK photons given the particular UHECR spectrum, would imply the emission of photons at the source or new physics. New physics is involved in Top-Down models, produced as an alternative to acceleration models to explain the origin of the highest energy cosmic rays. All Top-Down models predict photon dominance at the highest energies. If photons are not seen, Auger will place interesting bounds on production models.

The plan of the paper is the following. In Section II, we explain how we model the sources and the propagation of particles. In Section III, we calculate the maximum and minimum GZK photon fractions expected either with the AGASA spectrum or with the HiRes spectrum. In Section IV we show that very different cosmogenic neutrino fluxes could be associated with UHECR spectra with either minimum and maximum GZK photon fractions.

2. Modeling of the sources and particle propagation

We use a numerical code described in Ref. [33] to compute the flux of GZK photons produced by an homogeneous distribution of sources emitting originally only protons or nuclei. This is the same numerical code as in Ref. [26], with a few modifications.

The code uses the kinematic equation approach and calculates the propagation of nuclei, nucleons, stable leptons and photons using the standard dominant processes, explained for example in Ref. [34]). For nucleons, it takes into account single and multiple pion production and e^\pm pair production on the CMB, infrared/optical and radio backgrounds, neutron β -decays and the expansion of the Universe. For nuclei, it takes into account pion production, e^\pm pair production and photodissociation through scattering with infra-red and CMB photons. For photons, the code includes e^\pm pair production, $\gamma + \gamma_B \rightarrow e^+e^-$ and double e^\pm pair production $\gamma + \gamma_B \rightarrow e^+e^-e^+e^-$, processes. For electrons and positrons, it takes into account inverse Compton scattering, $e^\pm + \gamma_B \rightarrow e^\pm\gamma$, triple pair production, $e^\pm + \gamma_B \rightarrow e^\pm e^+e^-$, and synchrotron energy loss on extra galactic magnetic fields (EGMF). All these reactions are discussed in detail for example in the Ph.D. thesis of S. Lee [35] and that of O. Kalashev [33]. The propagation of nucleons and the electron-photon cascades are calculated self-consistently, namely secondary (and higher generation) particles arising in all reactions are propagated alongside the primaries. The hadronic interactions of nucleons are now derived from the well established SOPHIA event generator [36], more accurate in the multi-pion regime than the old code in Ref. [33]. For the photodisintegration coefficients of nuclei we use the approximation first introduced in Ref. [37] and then revised in Ref. [38]. As a check, we reproduce the energy loss length of iron obtained in Ref. [38] when using the same infrared-optical spectrum used in Ref. [38]. The simulation of the electron-photon cascade development was verified by detailed comparisons of its results with those obtained with an analogous code developed by an independent group [35]. It has already been used in a series of papers dedicated to cosmic rays and astrophysics [39, 40, 41, 15].

UHE particles lose their energy in interactions with the electro-magnetic background, which consists of CMB, radio, infra-red and optical (IRO) components, as well as EGMF. Protons are sensitive essentially to the CMB only, while for UHE photons and nuclei the radio and IRO components are respectively important, besides the CMB. Notice that the radio background is not yet well known and that our conclusions depend strongly on the background assumed. We include three models for the radio background: the background based on estimates by Clark *et al.* [42] and the two models of Protheroe

and Biermann [43], both predicting a larger background than the first. For the IRO background component we used the model of Ref. [44]. The infra-red and optical background is not important for the production of GZK photons from primary nucleons at high energies and their absorption. This background is important to transport the energy of secondary photons in the cascade process from the 0.1 - 100 TeV energy range to the 0.1-100 GeV energy range observed by EGRET, and the resulting flux in this energy range is not sensitive to details of the IRO background models. The IRO background is also important for the photodisintegration of nuclei, thus affects the photon fluxes predicted by models with sources emitting nuclei.

It is believed that the magnetic fields in clusters can be generated from a primordial “seed” if it has a comoving magnitude $B \sim 10^{-12}$ G [45, 8]. The evolution of the EGMF together with the large scale structure of the Universe has been simulated recently by two groups using independent numerical procedures [9, 8]. Magnetic field strengths significantly larger than 10^{-10} G were found only within large clusters of galaxies. In our simulations we vary the magnetic field strength in the range $B = 10^{-11} - 10^{-9}$ G, assuming an unstructured field along the propagation path.

Notice that if neutrons are produced at the sources, the results at high energies are identical to those obtained with protons. The interactions of neutrons and protons with the intervening backgrounds are identical and when a neutron decays practically all of its energy goes to the final proton (while the electron and neutrino are produced with energies 10^{17} eV or lower).

The resulting GZK photon flux depends on several astrophysical parameters. These parametrize the initial proton flux, the distribution of sources, the radio background and the EGMF. As it is usual, we take the spectrum of an individual UHECR source to be of the form:

$$F(E) = fE^{-\alpha} \Theta(E_{\max} - E) , \quad (1)$$

where f provides the flux normalization, α is the spectral index and E_{\max} is the maximum energy to which protons can be accelerated at the source.

We assume a standard cosmological model with a Hubble constant $H = 70 \text{ km s}^{-1} \text{ Mpc}^{-1}$, a dark energy density (in units of the critical density) $\Omega_{\Lambda} = 0.7$ and a dark matter density $\Omega_{\text{m}} = 0.3$. The total source density in this model can be defined by

$$n(z) = n_0(1+z)^{3+m} \Theta(z_{\max} - z)\Theta(z - z_{\min}) , \quad (2)$$

where m parameterizes the source density evolution, in such a way that $m = 0$ corresponds to non-evolving sources with constant density per comoving volume, and z_{\min} and z_{\max} are respectively the redshifts of the closest and most distant sources. We have fixed $m = 0$ in this paper (except in Fig. 9) because the high energy photons come from close by, thus the effect of the evolution of sources is small (we estimate that this may introduce an uncertainty of the order of 10% in the photon fluxes we find). Sources with $z > 2$ have a negligible contribution to the UHECR flux above 10^{18} eV.

We are implicitly assuming that the sources are astrophysical, since these are the only ones which could produce solely protons (or neutrons) and nuclei as UHECR primaries. Astrophysical acceleration mechanisms often result in $\alpha \gtrsim 2$ [46], however, harder spectra, $\alpha \lesssim 1.5$ are also possible, see e.g. Ref. [47]. In reality, the spectrum may differ from a power-law, it may even have a peak at high energies [48]. AGN cores could accelerate protons with induced electric fields, similarly to what happens in a linear accelerator, and this mechanism would produce an almost monoenergetic proton flux, with energies as high as 10^{20} eV or higher [49]. Here, we consider the power law index to be in the range $1 \leq \alpha \leq 2.7$. An injected proton spectrum with $\alpha \geq 2.5$ does not require an extra contribution to fit the UHECR data, except at very low energies $E < 10^{18}$ eV [50]. For $\alpha \leq 2$ an extra low energy component (LEC) is required to fit the UHECR data at $E < 10^{19}$ eV. The flux of super-GZK protons (and thus the flux of GZK photons too) depends strongly on the power law index α of the initial injected proton flux: it is lower for larger values of α . The dependence of the GZK photon flux on the maximum energy E_{\max} is more significant as α decreases. Here we will consider values of E_{\max} up to 10^{21} eV.

Most of the energy in GZK photons cascades down to below the pair production threshold for photons on the CMB and infrared backgrounds. In general, for $\alpha < 2$ the diffuse extragalactic gamma-ray flux measured by EGRET [51] at GeV energies may impose a constraint on the GZK photon flux at high energies, which we take into account and found not relevant for any of the models we study here.

The value of z_{\min} is connected to the density of sources. Quite often in the literature the minimal distance to the sources is assumed to be negligible (i.e. comparable to the interaction length). We also consider non-zero minimum distances of up to 50 Mpc (actually $z_{\min} = 0.01$), as inferred from the small-scale clustering of events seen in the AGASA data [52]. Contrary to AGASA, HiRes does not see a clustering component in its own data [53]. The combined dataset shows that clustering still exists, but it is not as significant as in the data of AGASA alone [54]. Note, that the non-observation of clustering in the HiRes stereo data does not contradict the result of AGASA, because of the small number of events in the sample [55]. Assuming proton primaries and a small EGMF (following Ref. [8]), it is possible to infer the density of the sources [56, 55] from the clustering component of UHECR. AGASA data alone suggest a source density of 2×10^{-5} Mpc $^{-3}$, which makes plausible the existence of one source within 25 Mpc of us. However, the HiRes negative result on clustering requires a larger density of sources and, as a result, a smaller distance to the nearest one of them. Larger values of the EGMF (as found in Ref. [9]), and/or some fraction of iron in the UHECR, have the effect of reducing the required number of sources and, consequently, increasing the expected distance to the nearest one.

3. Expected range of GZK photon fractions

In this section we estimate the maximum and minimum GZK photon flux expected if the UHECR spectrum is that of AGASA [3] or that HiRes [5]. We proceed using the method explained in Ref. [27].

As shown in Ref. [26], the largest GZK photon fractions in UHECR happen for small values of α , large values of E_{\max} , and small intervening backgrounds. The smallest GZK photon fluxes happen with the opposite choices. To take into account the effect of the intervening backgrounds, here we fit the UHECR data assuming either a maximal intervening background (the largest radio background of Protheroe and Biermann [43] and large EGMF, $B = 10^{-9}G$) or a minimal intervening background (the radio background of Clark *et al.* [42] and small EGMF, $B = 10^{-11}G$), with many different injected spectra. We assume the injected spectrum in Eq. 1, a uniform distribution of sources with a density as in Eq. 2 with $z_{\max} = 3$ and, to start with, $z_{\min} = 0$ and $m = 0$. We consider then many different spectra resulting from changing the slope α and the maximum energy E_{\max} in Eq. 1 within the ranges $1 \leq \alpha \leq 2.9$ and $10^{20}eV \leq E_{\max} \leq 1.3 \times 10^{21} eV$ in steps $\alpha_n = 1 + 0.1n$, with $n = 1$ to 19 and $E_\ell = Z \times 10^{19}eV \times 2^\ell$, with $\ell = 0$ to 10, where Z is the electric charge of the particle injected ($Z = 1$ for protons, but later we apply the same procedure to nuclei as well). For each one of the models so obtained we compute the predicted UHECR spectrum by summing up the contributions of protons plus GZK photons arriving to us from all sources.

In order to compare the predicted flux with the data, we take also into account the experimental error in the energy determination as proposed in Ref. [61]. We take a lognormal distribution for the error in the energy reconstructed by the experiment with respect to the true value of energy of the UHECR coming into the atmosphere. To find the expected flux we convolute the spectrum predicted by each model with the lognormal distribution in energy with the width given by the HiRes energy error $\Delta E/E = 17\%$ [5] and the AGASA energy error $\Delta E/E = 25\%$ [3] (the parameter σ in Eq. (5) of Ref. [61], the standard deviation of $\log_{10}E$, is $\sigma = (\Delta E/E)/\ln(10) \simeq (\Delta E/E)/2.3$). This procedure results in small but not negligible changes in the predicted spectra which are then compared to the observed spectrum. In particular, there are events predicted with energy larger than the maximum energy E_{\max} . Somewhat arbitrarily we consider the energy beyond which no event is predicted to be $(1 + 10\Delta E/E)E_{\max}$. Moreover, in the case of the AGASA spectrum, we take into account that there is a 1.2 factor between the energy of a photon event and the energy measured if the event is reconstructed assuming it is a proton [62, 63]. Thus we divide the energy of the predicted GZK photon energy by 1.2 before comparing it with the observed AGASA spectrum.

With each predicted spectrum we fit the UHECR data from $4 \times 10^{19} eV$ up to the last published bin of each spectrum (i.e. the 9 highest energy data bins of AGASA or the 12 highest energy bins of HiRes 1 and 2 combined monocular data) possibly plus one

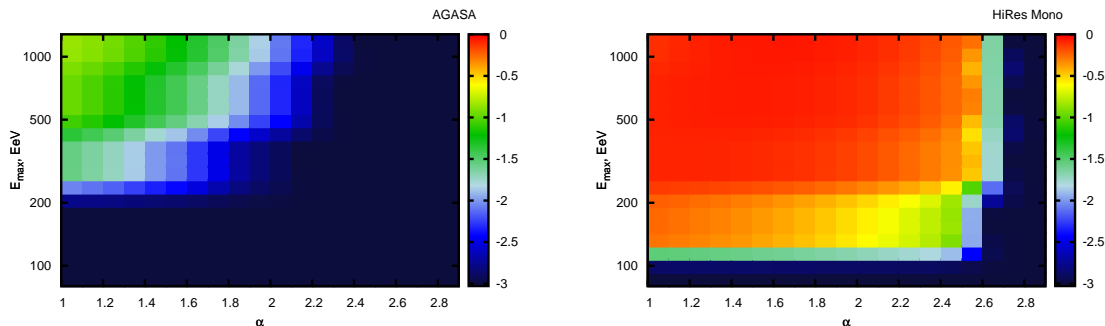


Figure 1. Color coded p -value plots as function of E_{\max} and α for the AGASA (left panel) and HiRes (right panel) spectra above 4×10^{19} eV. Figures look the same for maximum or minimum intervening radio background and EGMF. The color scale indicates the power index x where $p = 10^x$.

extra bin at higher energies. This last additional bin with zero observed events is added only if the maximum energy $(1 + 10\Delta E/E)E_{\max}$ (where E_{\max} is the maximum energy assumed for the injected spectrum in Eq. 1) is larger than the maximum energy of the last published bin (i.e. larger than 3.16×10^{20} eV for AGASA [3] and 3.98×10^{20} eV for HiRes [5]). This additional empty bin extends from the last published experimental point of each observed spectrum (which also are empty) to $(1 + 10\Delta E/E)E_{\max}$. We compute the expected number of events in this last bin using an exposure that we derive from the AGASA or HiRes data above 10^{20} eV and assuming the exposure is energy independent (above 10^{20} eV). This extra bin and the highest energy empty published bins, take into account the non-observation of events above the highest occupied energy bin in the data of each collaboration, the end-point energy of each spectrum (i.e. at $E > 2.3 \times 10^{20}$ eV for AGASA [3] and $E > 1.6 \times 10^{20}$ eV for HiRes [5]), although their aperture remains constant with increasing energy.

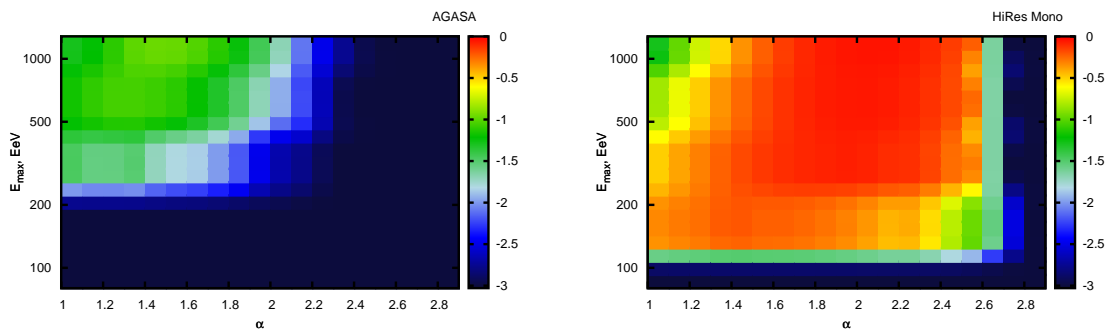


Figure 2. Same as Fig. 1 but maximizing the Poisson likelihood using UHECR data above 2×10^{19} eV instead of 4×10^{19} eV. Figures look the same for maximum or minimum intervening radio background and EGMF

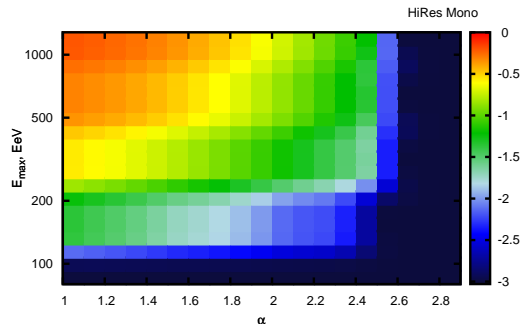


Figure 3. Same as Fig. 1 but for $z_{\min} = 0.01$ (instead of $z_{\min} = 0$) and only for the HiRes spectrum (there are no acceptable solutions for the AGASA spectrum). Figures look the same for maximum or minimum intervening radio background and EGMF

To fit the UHECR data with each predicted spectrum we follow a procedure similar to that of Ref. [57] applied to the bins just mentioned. The number of events and exposure data used to produce the latest published HiRes flux figures in Ref. [5] are given in Ref. [58]. For the AGASA spectrum, we reconstruct the measured number of events in each bin from the published data (using the error bars [59]). In both cases we compare the observed number of events in each bin with the number of events in each bin predicted by each one of the models. We choose the value of the parameter f in Eq. 1, i.e. the amplitude of the injected spectrum, by maximizing the Poisson likelihood function, which is equivalent to minimizing $-2 \ln \lambda$, (i.e. the negative of the log likelihood ratio) [60]. This procedure amounts to choosing the value of f so that the mean total number of events predicted (i.e. the sum of the average predicted number of events in all fitted bins) is equal to the total number of events observed. We then compute using a Monte Carlo technique the goodness of the fit, or p -value of the distribution, defined as the mean fraction of hypothetical experiments (observed spectra) with the same fixed total number of events which would result in a worse, namely lower, Poisson likelihood than the one obtained (in the maximization procedure that fixed f). These hypothetical experiments are chosen at random according to the multinomial distribution of the model (with f fixed as described). We have checked that this procedure when applied to bins with large number of events gives the same results as a Pearson's χ^2 fit, both for the value of the normalization parameter f and for the goodness of fit. A higher p value corresponds to a better fit, since more hypothetical experimental results would yield a worse fit than the one we obtained.

We make one additional requirement on the fit that insures that the predicted flux does not exceed the observed flux at energies below 4×10^{19} eV. We use the published fluxes at energies above 3×10^{18} eV for AGASA and 1.8×10^{17} eV for HiRes. For each assumed spectrum (with f fixed as described above) we calculate the χ^2 for the data at low energies only using the data points in which the predicted flux is above the observed flux (i.e. we take as zero the contribution to the χ^2 of each data point for which the

predicted flux is below the observed flux). We then require the p -value of the χ^2 so obtained to be larger than 0.05. This constraint eliminates the lowest values of α and E_{\max} . The regions eliminated by this requirement are assigned a p -value equal to zero in Figs. 1, 2 and 3.

Fig. 1 shows in a logarithmic scale the color coded p -value of the maximum Poisson likelihood value obtained for each model as function of E_{\max} and α for the AGASA (left panel) and HiRes (right panel) spectra. The figures look the same if they are produced with maximum or minimum intervening radio background and EGMF, because the contribution of GZK photons to the predicted spectra is always subdominant. In the case of AGASA we see that the best fits (those with larger p -values) occur at the largest α and E_{\max} we consider, and the fits are never very good: the p -value is never larger than 0.2. The best fits to the HiRes data can be better than the best fits to the AGASA data, the p -values can reach 0.7, and lie in a crescent-moon shaped region at more moderate values of α and E_{\max} .

The p -values obtained depend on the energy range chosen for the Poisson likelihood fit. In choosing to fit the data at energies 4×10^{19} eV and above without a low energy component (LEC) we are assuming that any LEC necessary to fit the spectrum at lower energies is negligible in this energy range. The goodness of the fit to the UHECR data depends on the lowest energy of the range we choose to fit, because the number of events in the lower energy bins is large. Had we chosen to fit the UHECR data from 2×10^{19} eV instead we would have obtained the p -values which we show in Fig. 2, just for comparison with Fig. 1. In Fig. 2 the region of best models moved to somewhat lower values of α and E_{\max} and their combined largest values (at the top left corner of the figure) are disfavored with respect to Fig. 1. We believe that a possible LEC may still be important to fit the UHECR data at 2×10^{19} eV. For example, iron would still be strongly deflected by the galactic magnetic fields up to energies to close to 3×10^{19} eV. Thus, a galactic iron component may be important up energies just below 4×10^{19} eV.

So far we have kept the minimum distance to the sources fixed to $z_{\min} = 0$. Fig. 3 shows the p -values obtained for $z_{\min} = 0.01$ (a minimum distance of 50 Mpc) through the same procedure for the HiRes spectrum. Fig. 3 shows that the allowed region of models for the HiRes spectrum moves to higher values of E_{\max} and α as z_{\min} increases. For the AGASA spectrum there are no allowed solutions within the range of E_{\max} and α we consider for $z_{\min} = 0.01$ or larger (the figure would look just black everywhere).

We proceed now to find the maximum and minimum GZK photon fractions. First, among all the models with $z_{\min} = 0, 0.00125, 0.0025, 0.005,$ and 0.01 (shown in Fig. 1 and Fig. 3 are only those with $z_{\min} = 0$ and 0.01 respectively) we chose those with p -value > 0.05 . Then, for these models we compute for a given E_{\max} the GZK photon fraction in the predicted integrated flux above a given energy E . Finally, we choose for each value of E_{\max} the values of α and z_{\min} for which the GZK photon fraction is either maximum and minimum. Figs. 4 and 5 show the maximum and minimum GZK photon fractions so obtained as a function of E_{\max} , for $z_{\min} = 0$, and variable z_{\min} in the range 0 to 0.01, respectively. We give the GZK photon fraction as a percentage of

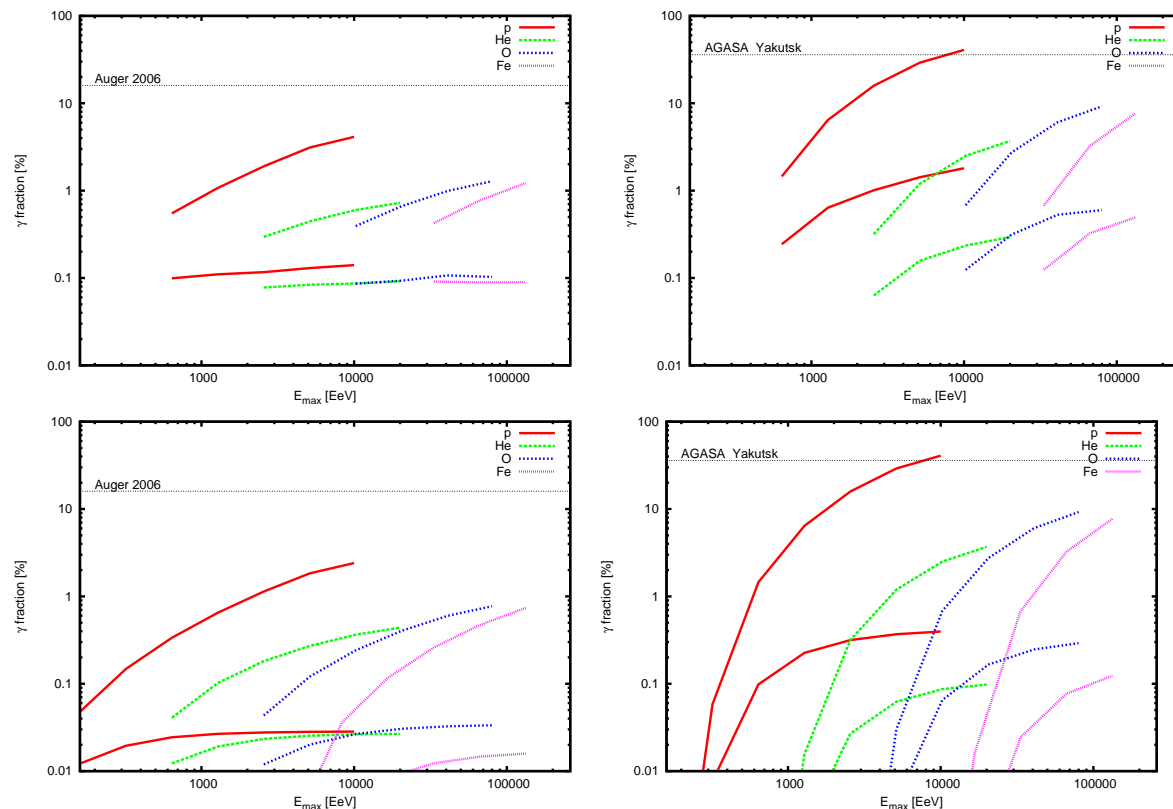


Figure 4. Maximum and minimum GZK photon fractions as function of E_{\max} between $Z \times 10^{20}$ eV and $Z \times 10^{22}$ eV, given in percentage of the integrated fluxes above $E = 1 \times 10^{19}$ eV (left panels) and 1×10^{20} eV (right panels) for AGASA (upper panels) and HiRes (lower panels) respectively, found among the models with p -value > 0.05 in Fig.1. Here we kept $z_{\min} = 0$. The colors indicate different primaries assumed: red for proton, green for He, blue for O and magenta for Fe.

the integrated flux above the energy E , for $E = 1 \times 10^{19}$ eV (left panels) and 1×10^{20} eV (right panels) for the AGASA spectrum (upper panels) and HiRes spectrum (lower panels) respectively. Notice that the ranges of GZK fractions do not change much with z_{\min} with the exception of the minimum photon fraction for HiRes above 1×10^{20} eV, which become much smaller for non zero z_{\min} . At 1×10^{19} eV the photon fractions are always larger than 10^{-4} . Figs. 4 and Fig. 5 also shows the experimental upper limits of the photon fraction obtained by Auger in 2006 [30] at energies above 1×10^{19} eV as well as the bound given by the Yakutsk collaboration combining data from Yakutsk and AGASA, above 1×10^{20} eV [63].

For comparison, we also include in Fig. 4 the range of photon fractions obtained following the same procedure, but assuming that either only He or only O or only Fe are emitted by the sources (even though these are not realistic models for the injected composition) and fitting the UHECR data with the processed products of photo-dissociation of the initial nuclei. The spectrum assumed for the nuclei is again as in Eq. 1 where E_{\max} is now the maximum energy of the injected nuclei. Here we consider E_{\max} between $Z \times 10^{20}$ eV and $Z \times 1 \times 10^{22}$ eV, where Z is the electric charge

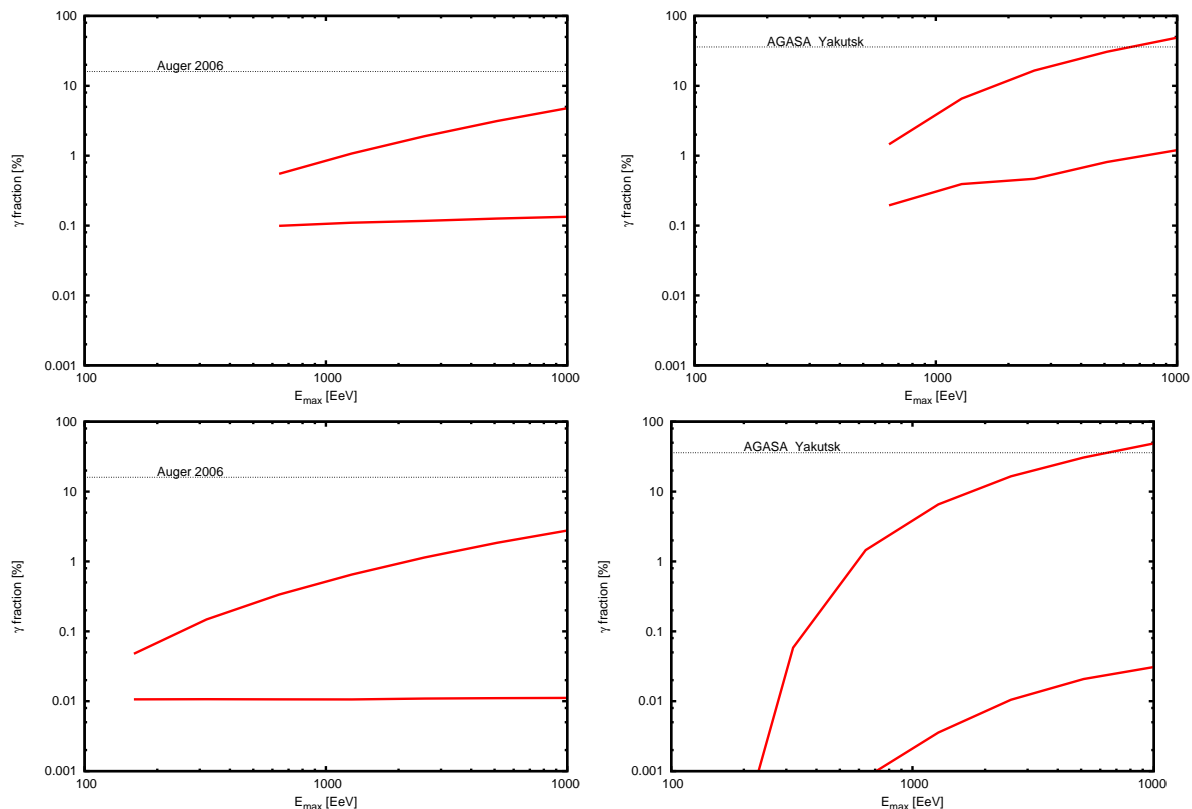


Figure 5. Maximum and minimum GZK photon fractions for proton primaries as function of E_{\max} between 1×10^{20} eV and 1.3×10^{21} eV, given in percentage of the integrated fluxes above $E = 1 \times 10^{19}$ eV (left panels) and 1×10^{20} eV (right panels) for AGASA (upper panels) and HiRes (lower panels) respectively, found among the models with p -value > 0.05 in Figs. 1 and 3. Here we allowed for variable z_{\min} between 0 and 0.01.

of each nucleus.

In Figs. 6 and 7 the maximum and minimum GZK photon fractions in the integrated flux above the energy E are shown as function of E for two values of E_{\max} , for fixed $z_{\min} = 0$ and for variable z_{\min} respectively. The GZK photon fraction is again given as a percentage of the integrated flux. The ranges of photon fraction do not change much with z_{\min} , except for the minimum fraction for HiRes. For comparison, we also include in Fig. 6 the results obtained following the same procedure, but assuming that either only He or only Fe are emitted by the sources, as explained above. The photon fractions are given for $E_{\max} = Z \times 10^{21}$ eV both for the AGASA (left) and the HiRes (right) spectrum. Upper bounds by Auger [30], Yakutsk [64] and AGASA-Yakutsk [63] are also shown. The maximum photon fractions produced by nuclei are not much smaller (within a factor of 2 to 10 smaller) that those of nucleons, but for Fe the minimum photon fractions can be much smaller (below 10^{-5}).

As an example of the fits we obtain to the observed spectra, in Fig 8 we show the differential flux of protons, of GZK photons and the total differential flux for two models which provide good fits to the HiRes UHECR spectrum either with maximal (left

panel) or with minimal (right panel) GZK photon fraction in the integrated flux above 1×10^{19} eV. In the figures z_{\min} was allowed to vary. The model with maximum GZK photon flux (left panel) has $z_{\min} = 0.00125$, $m = 0$, $E_{\max} = 1.3 \times 10^{21}$ eV, $\alpha = 1$ and minimal radio background and B ; the model with minimum photon content (right panel) has instead $z_{\min} = 0.005$, $m = 0$, $E_{\max} = 1.6 \times 10^{20}$ eV, $\alpha = 2$ and maximal radio background and B . In the left panel we show explicitly the effect of the intervening background, given the same source spectrum and distribution. The lower photon line in the left panel corresponds to the same source model as the higher photon line, but to intervening radio background and B field that are maximal instead of minimal. We clearly see that the uncertainty in the photon flux due solely to the intervening backgrounds is about one order of magnitude or less in this case. The fit to the HiRes data is the same because photons are in any event subdominant in the flux.

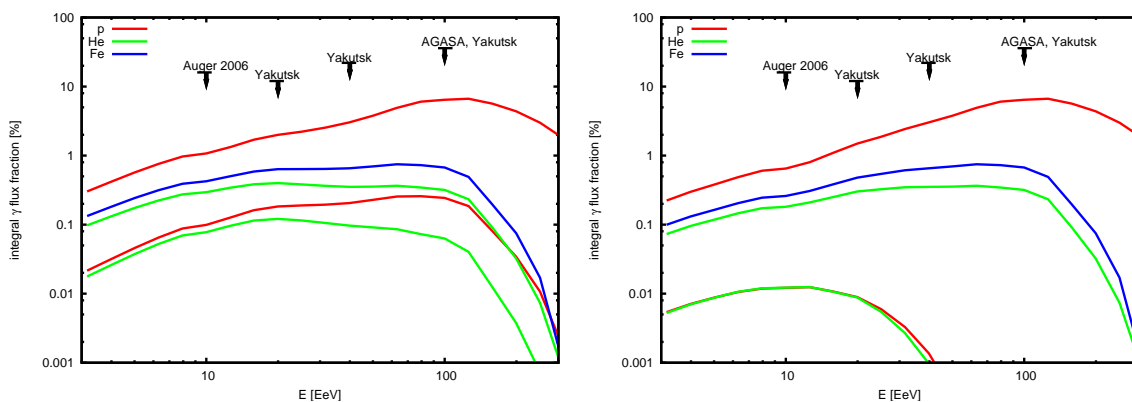


Figure 6. Maximum (higher lines) and minimum (lower lines) GZK photon fractions among models with fixed $z_{\min} = 0$, given as a percentage of the integrated fluxes above the energy E are shown as function of E for E_{\max} equal to $Z \times 1.28 \times 10^{21}$ eV, for AGASA (left) and HiRes (right). The colors indicate different primaries assumed: red for proton, green for He and blue for Fe. For Fe the minimum fractions are below the range shown in the figures.

4. Cosmogenic neutrinos

The GZK photons and cosmogenic neutrinos are due to the same photo-pion production mechanism: from the decay of π^0 we obtain GZK photons and from the decay of π^\pm one obtains neutrinos. These “cosmogenic neutrinos” have been extensively studied, from 1969 [13] onwards (see for example [14, 15] and references therein) and constitute one of the main high energy signals expected in neutrino telescopes, such as ICECUBE [16] ANITA [17] and SALSA [18] or space based observatories such as EUSO [19] and OWL [20].

Thus, GZK photons and cosmogenic neutrinos provide complementary information on the GZK effect. Although they share the same production mechanism GZK photons and cosmogenic neutrinos are affected very differently by intervening backgrounds. The flux of GZK photons is affected by the radio background and EGMF values which do

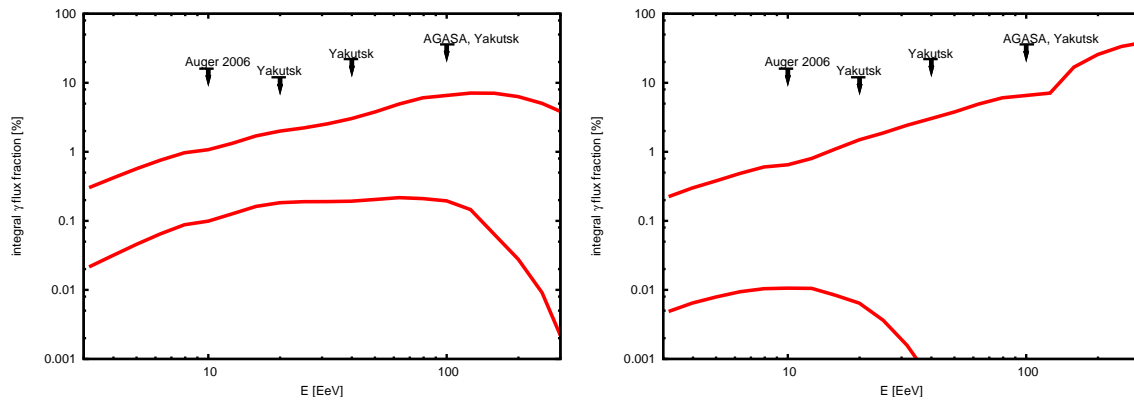


Figure 7. Maximum and minimum GZK photon fractions for proton primaries and z_{\min} varied between 0 and 0.01. Fractions given as a percentage of the integrated fluxes above the energy E are shown as function of E and E_{\max} equal to 1.28×10^{21} eV, for AGASA (left) and HiRes (right).

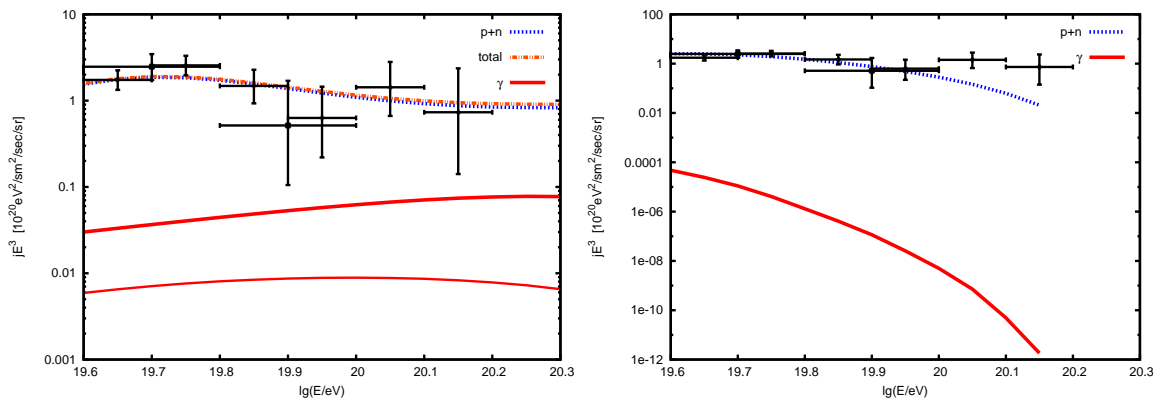


Figure 8. Differential proton, GZK photon and total fluxes which provide good fits to the HiRes spectrum for variable z_{\min} with either maximal (left panel) or minimal (right panel) GZK photon content. Left panel: $z_{\min} = 0.00125$, $m = 0$, $E_{\max} = 1.3 \times 10^{21}$ eV, $\alpha = 1$, minimal radio background and $B = 10^{-11}$ G for the higher photon line. Lower photon line in the left panel: same source model as higher line, except for maximal intervening radio background and $B = 10^{-9}$ G. Right panel: $z_{\min} = 0.005$, $m = 0$, $E_{\max} = 1.6 \times 10^{20}$ eV, $\alpha = 2$, maximal radio background and $B = 10^{-9}$ G.

not affect neutrinos. UHE GZK photons only reach us from less than 100 Mpc away, i.e. a redshift $z < 0.02$. Cosmogenic neutrinos do not interact during propagation and thus reach us from the whole production volume, which depends on the maximum redshift to the sources z_{\max} . Thus the flux of cosmogenic neutrinos arriving to Earth depends strongly on the evolution of the sources, which affect mostly the density of sources far away. The evolution in comoving volume is here parametrized by the power m , so that, excluding the Hubble expansion, the number density of sources is $\sim (1+z)^m$. In Fig. 9 we show six examples of cosmogenic neutrino fluxes for models which fit the HiRes spectrum with either maximum (left panel) or minimum (right panel) GZK photon fractions of integrated UHECR fluxes above $E = 1 \times 10^{19}$ eV, produced by protons emitted at the sources. These are the models of Fig. 8 (namely $E_{\max} = 1.3 \times 10^{21}$ eV, $\alpha = 1$, minimal

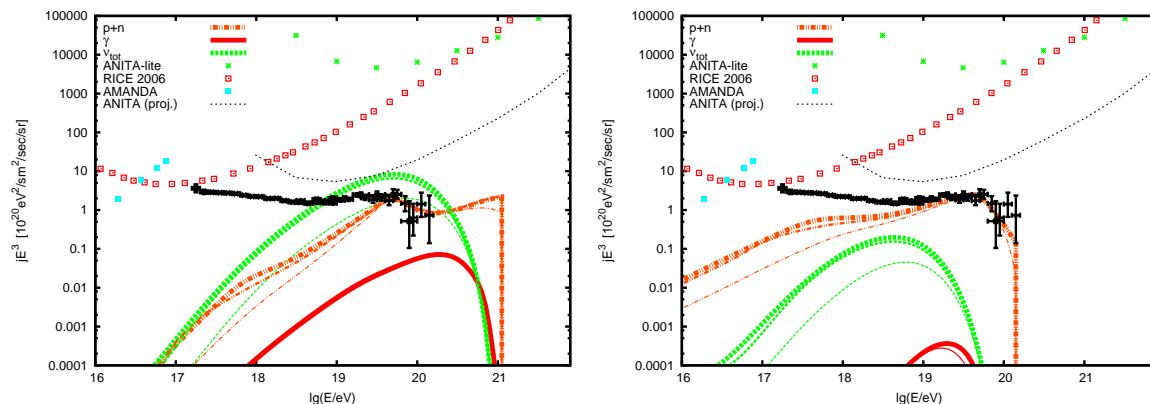


Figure 9. Cosmogenic neutrinos for models which fit the HiRes spectrum with maximum (left panel) and minimum (right panel) GZK photon fractions of the integrated UHECR fluxes above $E = 1 \times 10^{19}$ eV. Same models of Fig. 8 but for the three different source evolution models explained in the text.

radio background and $B = 10^{-11}$ G for the left panel and $E_{\max} = 1.6 \times 10^{20}$ eV, $\alpha = 2$, maximal radio background and $B = 10^{-9}$ G for the right panel) but assuming three particular source evolution models. The highest neutrino fluxes (thick lines) correspond to the fast star formation rate evolution model of Ref. [65] in which $m = 4$ from $z = 0$ to $z = 1$, then $(1+z)^m$ becomes constant (equal to $2^4 = 16$) from $z = 1$ to $z_{\max} = 6$ and then goes sharply to zero for $z > 6$. The intermediate neutrino fluxes (thinner dashed lines) correspond to an approximation to the evolution of radio galaxies and AGNs [66], which is somewhat faster than $m = 3$ below $z = 1$, peaks at about $z = 2$ and decreases rapidly in emissivity at $z > 3$. The approximation we used for the figures has $m = 3$ from $z = 0$ to $z = 1.8$, at which point $(1+z)^m$ becomes constant equal to $2.8^3 = 22$ up to $z_{\max} = 3$ where it goes sharply to zero for larger z . The lowest neutrinos fluxes in both panels (thinnest dashed lines) correspond to not evolving sources, i.e. $m = 0$, and $z_{\max} = 3$. The latter is an approximation to an older star population evolution and is taken here as a lower limit to the value of m at low redshifts. Negative values of m have been mentioned in the literature only for very massive clusters, which only formed recently. However, accretion shocks in clusters might accelerate heavy nuclei but not protons to the energies necessary to account for the ultrahigh energy cosmic rays [67].

The neutrino flux shown is the average flux per flavour, that is the total flux of neutrinos and antineutrinos divided by 3. Also shown in the figure are several upper bounds on cosmogenic neutrinos fluxes by ANITA-Light [68], AMANDA [69] and RICE [70] and the ANITA [17] projected bound.

Thick, intermediate and thin lines show the photon (solid red) and baryon p+n (dashed double dotted red lines) fluxes for the three source evolutions already mentioned. The baryon flux coincides with the total UHECR predicted, since photon fluxes are always subdominant.

Fig. 9 clearly shows that the different source evolution models assumed affect very little (left panel) or not at all (right panel) the GZK photon fluxes but yield different

cosmogenic neutrino neutrino fluxes. It is also clear from the figure that the cosmogenic neutrino fluxes are high when GZK photon fluxes are high and vice versa. We have not attempted here to maximize or minimize the cosmogenic neutrino fluxes, just to provide some examples of the expected range of fluxes given a particular GZK photon flux. Moreover, since here we fit the UHECR spectrum only above 4×10^{19} eV, we predict accurately the neutrino spectrum at energies above 4×10^{18} . At lower energies higher neutrino fluxes could be predicted if there is an extragalactic component to the UHECR at energies below 4×10^{19} eV.

5. Conclusions

The Pierre Auger Observatory has already set bounds on the photon fraction above 10^{19} eV [30] and better bounds are expected soon. We expect to have in the near future the high statistic data that may allow to study a subdominant component of UHECR consisting of photons. Auger will hopefully see photons or place a limit on the photon fraction at the level of a few % or below [29]. If complemented by an extended northern array, a sensitivity level of below 0.1% could be reached within a few years of full operation [29]. In this paper we address the physical implications of such detection or limits.

Here we calculate the flux of “GZK-photons”, namely the flux of photons produced by extragalactic nucleons through the resonant photoproduction of pions, the GZK effect. This flux depends on the UHECR spectrum on Earth, of the spectrum of nucleons emitted at the sources, which we characterize by its slope and maximum energy, on the distribution of sources and on the intervening cosmological backgrounds, in particular the magnetic field and radio backgrounds. We compute the possible range of the GZK photon fraction of the total UHECR flux for the AGASA and the HiRes spectra. We fit the UHECR data above 4×10^{19} eV either minimizing or maximizing the number of GZK protons produced. We find (see Figs. 6 and 7) that assuming exclusively nucleons are emitted at the sources the GZK photon fraction of the total integrated UHECR flux could reach a few % above 10^{19} eV and 10% above 10^{20} eV, or be between one (for AGASA) and several (for HiRes) orders of magnitude smaller, under the level that could be detected at Auger South. The maximum photon fractions do not depend much from the minimum distance to the sources.

We find (as in Ref. [27]) that the photon fraction in cosmic rays at energies above 10^{19} eV could be as low as 10^{-4} (Ref. [32] finds comparable small fractions). Photon fluxes so small could only be detected in future experiments like Auger North [31] plus South [29], EUSO [19] and OWL [20].

Just for comparison in Fig. 6 we also show the range of GZK-photon fractions expected if purely He or purely Fe nuclei were emitted at the sources, and in both cases the maximum GZK photon fractions expected are smaller by a factor between 2 and 10. For nuclei produced at the sources the maximum photon fraction is a factor of 2 to 3 times smaller above 10^{19} eV but the minimum could be much smaller than for nucleons.

The detection of UHECR photons would open a new window for ultra-high energy astronomy and help establish the UHECR sources. The detection of a larger photon flux than expected for GZK photons given the particular UHECR spectrum, would imply the emission of photons at the source or new physics, such as Top-Down models. If photons are not seen, Auger will place interesting bounds on GZK photon production models.

Finally we also briefly comment on cosmogenic neutrino fluxes, which provide complementary information on the GZK effect. Although they share the same production mechanism, GZK photons are affected by the radio background and EGMF which do not affect neutrinos and, contrary to photons, cosmogenic neutrinos depend strongly on the evolution of sources. In any event, as shown in Fig. 9, cosmogenic neutrino fluxes are high when GZK photon fluxes are high and vice versa.

Acknowledgments

The work of G.G and O.K. was supported in part by NASA grants NAG5-13399 and ATP03-0000-0057. G.G was also supported in part by the US DOE grant DE-FG03-91ER40662 Task C. The numerical part of this work was performed at the computer cluster of the INR RAS Theory Division and the “Neutrino” cluster of the UCLA Physics and Astronomy Department.

- [1] K. Greisen, Phys. Rev. Lett. **16**, 748 (1966). G. T. Zatsepin and V. A. Kuzmin, JETP Lett. **4**, 78 (1966) [Pisma Zh. Eksp. Teor. Fiz. **4**, 114 (1966)].
- [2] M. Takeda *et al.*, Phys. Rev. Lett. **81**, 1163 (1998); see N. Hayashida *et al.*, astro-ph/0008102, for an update; see also <http://www-akeno.icrr.u-tokyo.ac.jp/AGASA/>.
- [3] M. Takeda *et al.*, Astropart. Phys. **19**, 447 (2003) [astro-ph/0209422].
- [4] R. U. Abbasi *et al.* [High Resolution Fly’s Eye Collaboration], Phys. Rev. Lett. **92**, 151101 (2004); see also <http://hires.physics.utah.edu/>.
- [5] R. Abbasi *et al.* [HiRes Collaboration], astro-ph/0703099.
- [6] F.W. Stecker, Phys. Lett. **21**, 1016 (1968); S. Yoshida and M. Teshima, Prog. Theor. Phys. **89**, 833 (1993); F. A. Aharonian and J. W. Cronin, Phys. Rev. **D50**, 1892 (1994); J. W. Elbert and P. Sommers, Astrophys. J. **441**, 151 (1995);
- [7] F. Halzen, R. A. Vazquez, T. Stanev, and V. P. Vankov, Astropart. Phys., **3**, 151 (1995).
- [8] K. Dolag, D. Grasso, V. Springel and I. Tkachev, JETP Lett. **79**, 583 (2004) [Pisma Zh. Eksp. Teor. Fiz. **79**, 719 (2004)]; and JCAP **0501**, 009 (2005).
- [9] G. Sigl, F. Miniati and T. A. Ensslin, Phys. Rev. D **68**, 043002 (2003); astro-ph/0309695; Phys. Rev. D **70**, 043007 (2004); astro-ph/0409098.
- [10] V. Berezhinsky, A. Z. Gazizov and S. I. Grigorieva, hep-ph/0204357.
- [11] T. T. Stanev, Astrophys. J. **479**, 290 (1997); G. A. Medina-Tanco, E. M. de Gouveia Dal Pino and J. E. Horvath, astro-ph/9707041; M. Prouza and R. Smida, astro-ph/0307165.
- [12] Pierre Auger Observatory, <http://www.auger.org>.
- [13] V. S. Berezhinsky and G. T. Zatsepin, Phys. Lett **28B**, 423 (1969).
- [14] O. E. Kalashev, V. A. Kuzmin, D. V. Semikoz and G. Sigl, Phys. Rev. D **66**, 063004 (2002).
- [15] D. V. Semikoz and G. Sigl, JCAP **0404**, 003 (2004).
- [16] ICECUBE collaboration, <http://icecube.wis.edu/>.
- [17] ANtarctic Impulse Transient Array (ANITA), <http://www.ps.uci.edu/~anita/>.

- [18] Saltdome Shower Array, P. Gorham *et al.*, Nucl. Instrum. Meth. A **490**, 476 (2002).
- [19] Extreme Universe Space Observatory, <http://www.euso-mission.org/>. “JEM/EUSO Project” Talk by Inoue, I.; Ebisuzaki, E. on 6th COSPAR Scientific Assembly. Held 16 - 23 July 2006, in Beijing, China., p.2902.
- [20] Orbiting Wide-angle Light-collectors, <http://owl.gsfc.nasa.gov/>. F. W. Stecker *et al.* Nucl. Phys. Proc. Suppl. **136C**, 433 (2004).
- [21] J. Wdowczyk , W. Tkaczyk, C. Adcock and A. W. Wolfendale, J. Phys. A: Gen. Phys **4** L37-9 (1971); J. Wdowczyk , W. Tkaczyk and A. W. Wolfendale, J. Phys. A: Gen. Phys **5** 1419 (1972); J. Wdowczyk and A. W. Wolfendale, Astrophys. Jour. **349**, 35 (1990)
- [22] F.A. Aharonian, V.V. Vardanian and B.L. Kanevsky, Astrophysics and Space Science **167**, 111 (1990); *ibid* **93**, 111 (1990).
- [23] S. j. Lee, A. Olinto and G. Sigl, Astrophys. J. **455**, L21 (1995).
- [24] O. E. Kalashev, V. A. Kuzmin, D. V. Semikoz and I. I. Tkachev, astro-ph/0107130.
- [25] P. G. Tinyakov and I. I. Tkachev, JETP Lett. **74**, 445 (2001) [Pisma Zh. Eksp. Teor. Fiz. **74**, 499 (2001)].
- [26] G. Gelmini, O. Kalashev and D. V. Semikoz, astro-ph/0506128.
- [27] G. Gelmini, O. Kalashev and D. V. Semikoz, astro-ph/0702464.
- [28] X. Bertou, P. Billoir, and S. Dagoret-Campagne, Astropart. Phys. **14**, 121 (2000).
- [29] M. Risse and P. Homola, Mod. Phys. Lett. A **22**, 749 (2007).
- [30] J. Abraham *et al.* [Pierre Auger Collaboration], Astropart. Phys. **27**, 155 (2007).
- [31] Auger North web-site can be found here: <http://www.augernorth.org/>.
- [32] G. Sigl, Phys. Rev. D **75**, 103001 (2007).
- [33] O.E. Kalashev, V.A. Kuzmin and D.V. Semikoz, astro-ph/9911035. Mod. Phys. Lett. A **16**, 2505 (2001); O.E. Kalashev Ph.D. Thesis, INR RAS, 2003.
- [34] P. Bhattacharjee, G. Sigl, Phys. Rept. **327**, 109 (2000).
- [35] S. Lee, Phys. Rev. D **58**, 043004 (1998); G. Sigl, S. Lee and P. Coppi, astro-ph/9604093.
- [36] A. Mucke, R. Engel, J. P. Rachen, R. J. Protheroe and T. Stanev, Comput. Phys. Commun. **124**, 290 (2000).
- [37] J.L. Puget, F. W. Stecker and J. Bredekamp Astrophys. J. **205**, 638 (1976).
- [38] F. W. Stecker and M. H. Salamon, Astrophys. J. **512**, 521 (1999).
- [39] O. E. Kalashev, V. A. Kuzmin, D. V. Semikoz and G. Sigl, Phys. Rev. D **65** (2002) 103003.
- [40] A. Neronov, D. Semikoz, F. Aharonian and O. Kalashev, Phys. Rev. Lett. **89**, 051101 (2002).
- [41] O. E. Kalashev, V. A. Kuzmin, D. V. Semikoz and G. Sigl, Phys. Rev. D **66**, 063004 (2002).
- [42] T. A. Clark, L. W. Brown, and J. K. Alexander, Nature **228**, 847 (1970).
- [43] R. J. Protheroe and P. L. Biermann, Astropart. Phys. **6**, 45 (1996) [Erratum-*ibid.* **7**, 181 (1997)]
- [44] F. W. Stecker, M. A. Malkin and S. T. Scully, Astrophys. J. **648**, 774 (2006).
- [45] K. Dolag, M. Bartelmann and H. Lesch, Astron. & Astrophys. **387**, 383 (2002).
- [46] V. S. Berezinsky, et al, “*Astrophysics of Cosmic Rays.*” (North-Holland, Amsterdam, 1990); T.K. Gaisser, “*Cosmic Rays and Particle Physics.*” (Cambridge University Press, Cambridge, England, 1990).
- [47] R.J. Protheroe, In “*Topics in cosmic-ray astrophysics*”, ed. M. A. DuVernois, Nova Science Publishing: New York, 1999, (astro-ph/9812055); M.A. Malkov, Ap.J. **511**, L53 (1999); K. Mannheim, R.J. Protheroe, J. P. Rachen, Phys. Rev. **D63**, 023003 (2001).
- [48] E. V. Derishev, F. A. Aharonian, V. V. Kocharovskiy and V. V. Kocharovskiy, Phys. Rev. D **68**, 043003 (2003).
- [49] A. Neronov and D. Semikoz, New Astronomy Reviews **47**, 693 (2003); A. Neronov, P. Tinyakov and I. Tkachev, J. Exp. Theor. Phys. **100**, 656 (2005) [Zh. Eksp. Teor. Fiz. **100**, 744 (2005)] [astro-ph/0402132].
- [50] V. Berezinsky, A. Gazizov and S. Grigorieva, astro-ph/0210095; Phys. Lett. B **612**, 147 (2005).
- [51] P. Sreekumar *et al.* [EGRET Collaboration], Astrophys. J. **494**, 523 (1998).
- [52] M. Takeda *et al.*, Astrophys. J. **522**, 225 (1999).

- [53] R. U. Abbasi *et al.* [HIRES], *Astrophys. J.* **610**, L73 (2004). [astro-ph/0404137].
- [54] R. U. Abbasi *et al.* [The High Resolution Fly’s Eye Collaboration (HIRES)], astro-ph/0412617.
- [55] H. Yoshiguchi, S. Nagataki and K. Sato, *Astrophys. J.* **614**, 43 (2004); M. Kachelriess and D. Semikoz, *Astropart. Phys.* **23**, 486 (2005).
- [56] E. Waxman, K. B. Fisher and T. Piran, *Astrophys. J.* **483**, 1 (1997); S. L. Dubovsky, P. G. Tinyakov and I. I. Tkachev, *Phys. Rev. Lett.* **85**, 1154 (2000); Z. Fodor and S. D. Katz, *Phys. Rev. D* **63**, 023002 (2001); H. Yoshiguchi, S. Nagataki, S. Tsubaki and K. Sato, *Astrophys. J.* **586**, 1211 (2003) [Erratum-ibid. **601**, 592 (2004)]; H. Yoshiguchi, S. Nagataki and K. Sato, *Astrophys. J.* **592**, 311 (2003); P. Blasi and D. De Marco, *Astropart. Phys.* **20**, 559 (2004).
- [57] Z. Fodor, S. D. Katz and A. Ringwald, *Phys. Rev. Lett.* **88**, 171101 (2002) and *JHEP* **0206**, 046 (2002).
- [58] <http://www.physics.rutgers.edu/%7Edbergman/HiRes-Monocular-Spectra-200702.html>
- [59] G. Cowan “Statistical data analysis”, Oxford University Press, 1998, Section 9.4.
- [60] S. Baker and R.D. Cousins, *Nucl. Instrum. Methods* **221**, 437 (1984); Particle Data Group’s Statistics Review (2004).
- [61] I. F. M. Albuquerque and G. F. Smoot, *Astropart. Phys.* **25**, 375 (2006).
- [62] P. Homola *et al.*, *Nucl. Phys. Proc. Suppl.* **151** (2006) 119; M. Risse *et al.*, *Phys. Rev. Lett.* **95**, 171102 (2005).
- [63] G. I. Rubtsov *et al.*, *Phys. Rev. D* **73**, 063009 (2006).
- [64] A. V. Glushkov *et al.* *JETP Lett.* **85**, 131 (2007).
- [65] F. W. Stecker, M. A. Malkan and S. T. Scully, *Astrophys. J.* **648**, 774 (2006).
- [66] J. S. Dunlop and J. A. Peacock, *MNRAS* **247**, 19 (1990).
- [67] S. Inoue, G. Sigl, F. Miniati and E. Armengaud, astro-ph/0701167.
- [68] S. W. Barwick *et al.* [ANITA Collaboration], *Phys. Rev. Lett.* **96**, 171101 (2006).
- [69] M. Ackermann *et al.* [AMANDA Collaboration], *Astropart. Phys.* **22**, 127 (2004).
- [70] A. Bean [RICE Collaboration], *AIP Conf. Proc.* **870** (2006) 212.